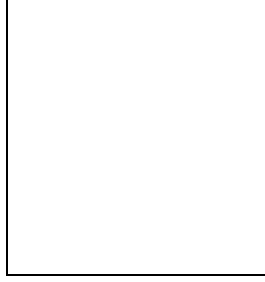


Overview of flavour physics with focus on the MSSM and 2HDMs

ANDREAS CRIVELLIN

CERN Theory Division, CH-1211 Geneva 23, Switzerland



In these proceedings we give a concise review of some selected flavour-violation processes and their implications for two-Higgs-doublet models (2HDMs) and the MSSM. The processes under investigation are $\Delta F = 2$ processes, $B_s \rightarrow \mu^+ \mu^-$, $b \rightarrow s\gamma$, and tauonic B decays. For each process we show the impact on the models.

1 Introduction

In recent years flavour physics has been one of the most active and fastest developing fields in high energy physics. Numerous new experiments were carried out but almost all of them reported result in agreement with the Standard Model (SM) predictions. There are only a few exceptions like the anomaly in the anomalous magnetic moment of the muon or recently the deviations from the SM predictions in tauonic B decays¹ and $B \rightarrow K^* \mu^+ \mu^-$ ².

The extensive set of measurements available for rare decays puts strong constraints on the flavour structure of physics beyond the Standard Model, in particular, on the flavour- and CP-violating parameters of the Minimal Supersymmetric Standard Model (MSSM) (see for example³ for an overview) or the two-Higgs doublet model (2HDM)⁴.

The SM has only one Higgs doublet and in a 2HDM (which is the decoupling limit of the MSSM) we introduce a second Higgs doublet and obtain four additional physical Higgs particles (in the case of a CP conserving Higgs potential): the neutral CP-even Higgs H^0 , a neutral CP-odd Higgs A^0 and the two charged Higgses H^\pm . In addition, if we allow for a generic flavour structure we have the non-holomorphic couplings which couple up (down) quarks to the down (up) type Higgs doublet: $\bar{u}_f \epsilon_{fi}^u u_i H^d$ and $d_f \epsilon_{fi}^d d_i H^u$ where ϵ_{ij}^q parametrizes the completely flavour-chaining neutral currents.

In the MSSM at tree-level $\epsilon_{ij}^q = 0$ (which corresponds to the 2HDM of type II) and flavour changing neutral Higgs couplings are absent. However, these couplings are generated at the loop level. The resulting expressions are non-decoupling and depend only on the ratios of SUSY parameters (for a complete one-loop analysis see⁵ and for the 2-loop SQCD corrections⁶).

2 Selected flavour-processes and their implications

2.1 $\Delta F = 2$ processes

$\Delta F = 2$ processes are still one of the most constraining processes for NP (see⁷ for an overview on $B_q - \bar{B}_q$ mixing) since they scale like δ^2/Λ^2 while the other flavour observables scale like δ/Λ^2 . Here δ stands for a generic flavour violating parameter and Λ is the scale of NP. Especially

the constraints from Kaon and D mixing are very stringent. They can be used for example to constrain the mass splitting of left-handed squarks in the MSSM⁸ (see left plot of Fig. 1).

2.2 $B_q \rightarrow \mu^+ \mu^-$

Thanks to LHCb and CMS⁹ we know the branching ratio for $B_s \rightarrow \mu^+ \mu^-$ now rather precisely and also the SM prediction has been improved recently¹⁰:

$$\text{Br}[B_s \rightarrow \mu^+ \mu^-]_{\text{exp}} = (2.9 \pm 0.7) \times 10^{-9}, \quad \text{Br}[B_s \rightarrow \mu\mu]_{SM} = (3.65 \pm 0.23) \times 10^{-9}. \quad (1)$$

Due to the good agreement with the SM we can place stringent bounds on models of NP, especially if they have sizable flavour-changing scalar currents like the generic 2HDM or the MSSM at large $\tan\beta$. In the middle plot of Fig. 1 we show the constraints on the 2HDM parameter $\epsilon_{23,32}^d$ which generate $B_s \rightarrow \mu^+ \mu^-$ via a tree-level Higgs exchange.

While the experimental bounds on $B_d \rightarrow \mu^+ \mu^-$ are still weaker due to the further CKM suppressed SM contribution LHCb will further improve experimental limit in the future. Also here stringent limits on $\epsilon_{13,31}^d$ can be obtained and similarly $K_L \rightarrow \mu^+ \mu^-$ and $D \rightarrow \mu^+ \mu^-$ but bounds on $\epsilon_{12,21}^q$. In summary, neutral meson decays to muons constrain all flavour-changing elements ϵ_{ij}^d and $\epsilon_{12,21}^u$ stringently.

2.3 $b \rightarrow q\gamma$

Concerning the radiative B decays $b \rightarrow s\gamma$ and $b \rightarrow d\gamma$ the current experimental values and theoretical predictions are given by:

$$\begin{aligned} \text{Br}[b \rightarrow s\gamma]_{\text{exp}} &= (3.43 \pm 0.21 \pm 0.07) \times 10^{-4}, & \text{Br}[b \rightarrow s\gamma]_{SM} &= (3.13 \pm 0.22) \times 10^{-4}, \\ \text{Br}[b \rightarrow d\gamma]_{\text{exp}} &= (1.41 \pm 0.57) \times 10^{-5}, & \text{Br}[b \rightarrow d\gamma]_{SM} &= 1.54_{-0.31}^{+0.26} \times 10^{-5}. \end{aligned} \quad (2)$$

Again, we observe a good agreement between theory predictions^a and experiment. $b \rightarrow s\gamma$ can for example be used to put bounds on ϵ_{23}^u originating from charged Higgs loop contributions. The results are shown in the right plot of Fig. 1. Similar constraints apply for ϵ_{13}^u from $b \rightarrow d\gamma$.

2.4 Tauonic B decays

Tauonic B -meson decays are an excellent probe of new physics: they test lepton flavor universality satisfied in the SM and are sensitive to new particles which couple proportionally to the mass of the involved particles (e.g. Higgs bosons) due to the heavy τ lepton involved. Recently, the BABAR collaboration performed an analysis of the semileptonic B decays $B \rightarrow D\tau\nu$ and $B \rightarrow D^*\tau\nu$ using the full available data set¹. They find for the ratios

$$\mathcal{R}(D^{(*)}) = \mathcal{B}(B \rightarrow D^{(*)}\tau\nu)/\mathcal{B}(B \rightarrow D^{(*)}\ell\nu), \quad (3)$$

the following results:

$$\mathcal{R}(D) = 0.440 \pm 0.058 \pm 0.042, \quad \mathcal{R}(D^*) = 0.332 \pm 0.024 \pm 0.018. \quad (4)$$

Here the first error is statistical and the second one is systematic. Comparing these measurements to the SM predictions

$$\mathcal{R}_{SM}(D) = 0.297 \pm 0.017, \quad \mathcal{R}_{SM}(D^*) = 0.252 \pm 0.003, \quad (5)$$

^aThe SM prediction for $b \rightarrow d\gamma$ is taken from¹¹ while the value for $b \rightarrow s\gamma$ is a preliminary result presented in Portoroz 2013 by Mikolaj Misiak.

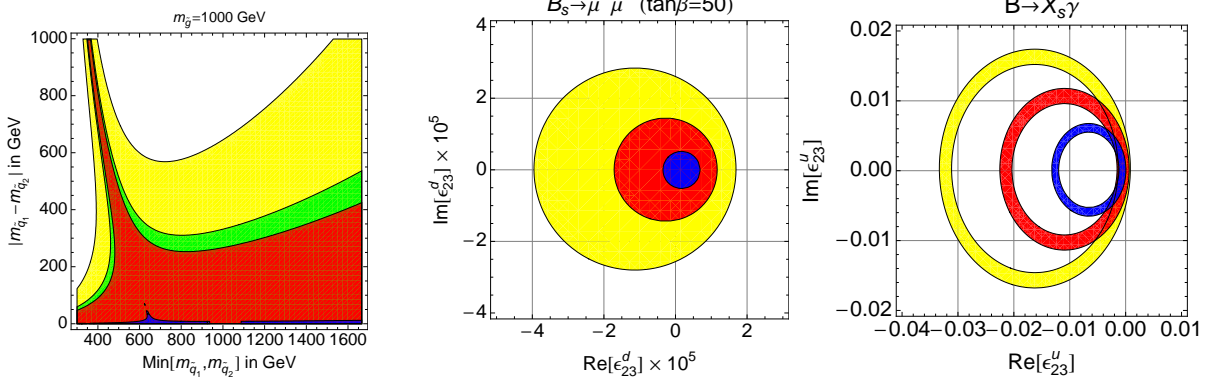


Figure 1: Left: Allowed mass splitting between the first two generations of left-handed squarks for different gluino masses for $M_2 = (\alpha_2/\alpha_s)m_{\tilde{g}} \cong 0.35$. Yellow (lightest) corresponds to the maximally allowed mass splitting assuming an intermediate alignment of $m_{\tilde{q}}^2$ with $Y_u^\dagger Y_u$ and $Y_d^\dagger Y_d$. The green (red) region is the allowed range assuming an diagonal up (down) squark mass matrix. The blue (darkest) area is the minimal region allowed in which the off-diagonal element carries a maximal phase. Middle: Allowed regions in the complex ϵ_{23}^d -plane from $B_s \rightarrow \mu^+ \mu^-$ for $\tan \beta = 50$ and $m_H = 700$ GeV (yellow), $m_H = 500$ GeV (red) and $m_H = 300$ GeV (blue). Note that the allowed regions for ϵ_{32}^d -plane are not full circles because in this case a suppression of $\mathcal{B}[B_s \rightarrow \mu^+ \mu^-]$ below the experimental lower bound is possible. Right: Allowed regions for ϵ_{23}^u from $B \rightarrow X_s \gamma$, obtained by adding the 2σ experimental error and theoretical uncertainty linear for $\tan \beta = 50$ and $m_H = 700$ GeV (yellow), $m_H = 500$ GeV (red) and $m_H = 300$ GeV (blue).

we see that there is a discrepancy of 2.2σ for $\mathcal{R}(\mathcal{D})$ and 2.7σ for $\mathcal{R}(\mathcal{D}^*)$ and combining them gives a 3.4σ deviation from the SM¹. This evidence for new physics in B -meson decays to taus is further supported by the measurement of $\mathcal{B}[B \rightarrow \tau \nu] = (1.15 \pm 0.23) \times 10^{-4}$ which disagrees with by 1.6σ higher than the SM prediction using V_{ub} from a global fit of the CKM matrix¹².

A natural possibility to explain these enhancements compared to the SM prediction is a charged scalar particle which couples proportionally to the masses of the fermions involved in the interaction: a charged Higgs boson. A charged Higgs affects $B \rightarrow \tau \nu$ ¹³, $B \rightarrow D \tau \nu$ and $B \rightarrow D^* \tau \nu$ ¹⁴. In a 2HDM of type II (with MSSM like Higgs potential) the only free additional parameters are $\tan \beta = v_u/v_d$ (the ratio of the two vacuum expectation values) and the charged Higgs mass m_{H^\pm} (the heavy CP even Higgs mass m_{H^0} and the CP odd Higgs mass m_{A^0} can be expressed in terms of the charged Higgs mass and differ only by electroweak corrections). In this setup the charged Higgs contribution to $B \rightarrow \tau \nu$ interferes necessarily destructively with the SM contribution¹³. Thus, an enhancement of $\mathcal{B}[B \rightarrow \tau \nu]$ is only possible if the absolute value of the charged Higgs contribution is bigger than two times the SM one^b. Furthermore, a 2HDM of type II cannot explain $\mathcal{R}(\mathcal{D})$ and $\mathcal{R}(\mathcal{D}^*)$ simultaneously¹.

As we found before, all ϵ_{ij}^d and $\epsilon_{13,23}^u$ are stringently constrained from FCNC processes in the down sector and only ϵ_{31}^u (ϵ_{32}^u) significantly effects $B \rightarrow \tau \nu$ ($\mathcal{R}(\mathcal{D})$ and $\mathcal{R}(\mathcal{D}^*)$) without any suppression by small CKM elements. Furthermore, since flavor-changing top-to-up (or charm) transitions are not measured with sufficient accuracy, we can only constrain these elements from charged Higgs-induced FCNCs in the down sector. However, since in this case an up (charm) quark always propagates inside the loop, the contribution is suppressed by the small Yukawa couplings of the up-down-Higgs (charm-strange-Higgs) vertex involved in the corresponding diagrams. Thus, the constraints from FCNC processes are weak, and $\epsilon_{32,31}^u$ can be sizable. Indeed, it turns out that by using $\epsilon_{32,31}^u$ we can explain $\mathcal{R}(\mathcal{D}^*)$ and $\mathcal{R}(\mathcal{D})$ simultaneously¹⁶. In Fig. 2 we see the allowed region in the complex ϵ_{32}^u -plane, which gives the correct values for $\mathcal{R}(\mathcal{D})$ and $\mathcal{R}(\mathcal{D}^*)$ within the 1σ uncertainties for $\tan \beta = 50$ and $M_H = 500$ GeV. Similarly, $B \rightarrow \tau \nu$ can be explained by using ϵ_{31}^u .

^b Another possibility to explain $B \rightarrow \tau \nu$ is the introduction of a right-handed W -coupling¹⁵.

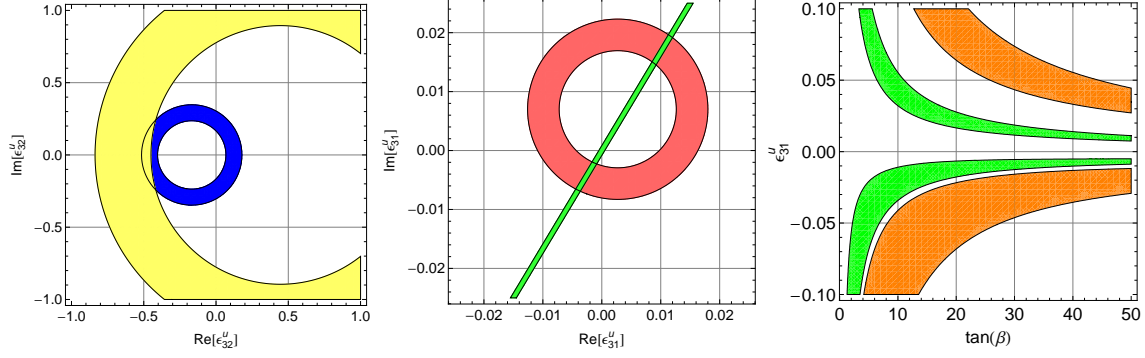


Figure 2: Left: Allowed regions in the complex ϵ_{32}^u -plane from $\mathcal{R}(\mathcal{D})$ (blue) and $\mathcal{R}(\mathcal{D}^*)$ (yellow) for $\tan\beta = 50$ and $m_H = 500$ GeV. Middle: Allowed regions in the complex ϵ_{31}^u -plane from $B \rightarrow \tau\nu$. Right: Allowed regions in the $\tan\beta$ - ϵ_{31}^u plane from $B \rightarrow \tau\nu$ for real values of ϵ_{31}^u and $m_H = 400$ GeV (green), $m_H = 800$ GeV (orange). The scaling of the allowed region for ϵ_{32}^u with $\tan\beta$ and m_H is the same as for ϵ_{31}^u . ϵ_{32}^u and ϵ_{31}^u are given at the matching scale m_H .

Acknowledgments

I thank the organizers, especially Maria Krawczyk, for the invitation and the possibility to present these results. This work is supported by a Marie Curie Intra-European Fellowship of the European Community's 7th Framework Programme under contract number (PIEF-GA-2012-326948).

1. J. P. Lees *et al.* [BaBar Collaboration], Phys. Rev. Lett. **109** (2012) 101802 [arXiv:1205.5442 [hep-ex]].
2. RAaij *et al.* [LHCb Collaboration], Phys. Rev. Lett. **111** (2013) 191801 [arXiv:1308.1707 [hep-ex]].
3. W. Altmannshofer, A. J. Buras, S. Gori, P. Paradisi and D. M. Straub, Nucl. Phys. B **830** (2010) 17 [arXiv:0909.1333 [hep-ph]].
4. A. Crivellin, A. Kokulu and C. Greub, Phys. Rev. D **87** (2013) 9, 094031 [arXiv:1303.5877 [hep-ph]].
5. A. Crivellin, L. Hofer and J. Rosiek, JHEP **1107** (2011) 017 [arXiv:1103.4272 [hep-ph]].
6. A. Crivellin and C. Greub, Phys. Rev. D **87** (2013) 015013 [arXiv:1210.7453 [hep-ph]].
7. A. Lenz, U. Nierste, J. Charles, S. Descotes-Genon, A. Jantsch, C. Kaufhold, H. Lacker and S. Monteil *et al.*, Phys. Rev. D **83** (2011) 036004 [arXiv:1008.1593 [hep-ph]].
8. A. Crivellin and M. Davidkov, Phys. Rev. D **81** (2010) 095004 [arXiv:1002.2653 [hep-ph]].
9. RAaij *et al.* [LHCb Collaboration], Phys. Rev. Lett. **110** (2013) 021801 [arXiv:1211.2674 [hep-ex]]. S. Chatrchyan *et al.* [CMS Collaboration], Phys. Rev. Lett. **111** (2013) 101804 [arXiv:1307.5025 [hep-ex]]. R. Aaij *et al.* [LHCb Collaboration], Phys. Rev. Lett. **111** (2013) 101805 [arXiv:1307.5024 [hep-ex]]. CMS and LHCb Collaborations [CMS and LHCb Collaboration], CMS-PAS-BPH-13-007.
10. C. Bobeth, M. Gorbahn, T. Hermann, M. Misiak, E. Stamou and M. Steinhauser, Phys. Rev. Lett. **112** (2014) 101801 [arXiv:1311.0903 [hep-ph]].
11. A. Crivellin and L. Mercolli, Phys. Rev. D **84** (2011) 114005 [arXiv:1106.5499 [hep-ph]].
12. J. Charles *et al.* [CKMfitter Group Collaboration], Eur. Phys. J. C **41** (2005) 1 [hep-ph/0406184].
13. W. -S. Hou, Phys. Rev. D **48** (1993) 2342.
14. M. Tanaka, Z. Phys. C **67** (1995) 321 [hep-ph/9411405].
15. A. Crivellin, Phys. Rev. D **81** (2010) 031301 [arXiv:0907.2461 [hep-ph]].
16. A. Crivellin, C. Greub and A. Kokulu, Phys. Rev. D **86** (2012) 054014 [arXiv:1206.2634 [hep-ph]].